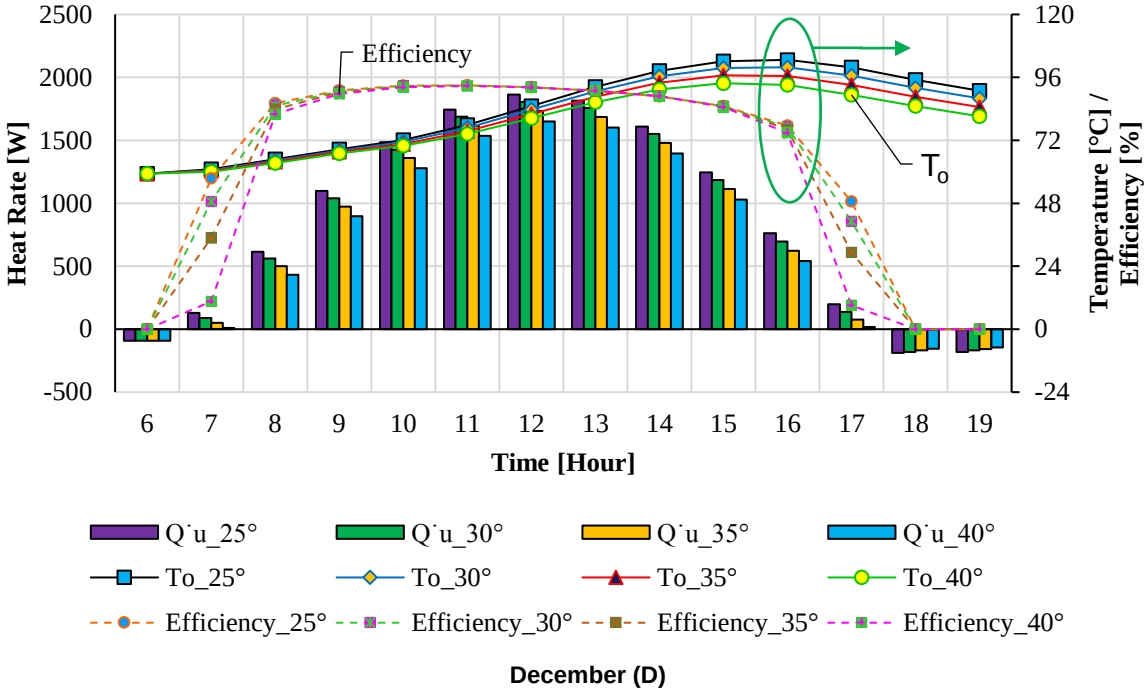

Figure 8: Collector slope performance trends for March, June, September and December.

From these figures, the trends are similar at different tilt angles during the seasons, but vary in the potential amount absorbed. This can be traced back to the solar angle relations in the sky model, in which the two-degree movement of the sun in its celestial orbit plays a crucial role. On 21 March (autumn) and 21 September (spring), the irradiance incident angle on the surface of the collector slopes are close to equilibrium and geometric factors are equal. This results in the amount of absorbed heat to be similar, respective to the season. In addition, given that the absorbed amount of heat is similar for all the slope angles in the specific season, the temperature and efficiency should rise, peak and fall accordingly with minor differences. An observation of the yearly solstices, 21 December and 21 June, shows that the amount of heat increases and decreases stepwise in relation to the slope angle. The incidence angles on the surface of the collector vary with the slopes angles, and as such are related to the largest and smallest angles to use in these seasons. Considering the dependence of incident angle on the heat absorption, as previously discussed, an inference can be made about the relationship between the two variables. For a system producing service-water, in summer, the slope of 40° is found to produce the least amount of useful heat and outlet temperature, whereas a slope of 25° produces the most. However, the precise opposite is found in winter, when 40° slope produces the most. The same inverse seasonal relationships are found for slope angles of 35° and 30°. Nonetheless, this provide an insight into optimal performance prediction during the year. The capacitance is significantly affected by the service–water demand in such a way that the capacitance is insufficient for temperature rises in the early-morning and afternoon hours. These are the hours of highest demand, resulting in the inability of the system to comply with the required output. In periods of low demand, the system temperature increases despite the steady decrease of absorbed radiation. This is due to the tank capacitance being higher than the demand requirement in these time periods. The collectors' capacity to absorb the incoming heat in morning and afternoon hours is limited to the available irradiation. As such, when little to no irradiance is available, the collector emits higher internal manifold working fluid heat to the colder environment. Similarly, the consumption rate at these hours assists in preventing useful heat gain to increase. These factors that limit heat gain cause the thermal efficiency to be zero in these periods. However, in periods of abundant irradiance, the efficiency quickly increases, reaches a peak and decreases due to its dependency on the temperature differences of the manifold's inlet and outlet. Intrinsically, the collectors' temperatures are dependent on the tank temperature that supply the collectors' manifold. The tank temperature that supplies the manifold is confined to the

simple system model expression. As such, as the useful heat surpasses the consumption loads and heat losses from the components, the inlet temperature to the next collector loop increases. If the consumption loads overwhelm the useful heat, the tank temperature will decrease, thereby decreasing the next collector loop inlet temperature. When irradiation is abundant and demand is low, the inlet and outlet temperatures of the collector will, therefore, increase. When the inlet temperature of the collector increases over time, however, the temperature difference of the collector will decrease. The tank temperatures and storage quantities can be visualised as in Figure 9. Examining the optimum output parameters for the different slope angles, as shown in Table 2, an inference can be made regarding the optimal slope angle.

The maximum temperature obtained is close to scalding and, therefore, utilising only one tank can be seen as dangerous. A multi-tank system can control the required temperature to be supplied to the occupants, making it the favourable choice. The system is pressurised at 400 kPa and the stagnation temperature is 143.65 °C, therefore the working fluid is also still in a liquid state at the higher obtainable temperatures. The efficiency in this study is defined as the ratio of useful heat to the absorbed irradiance. This will result in higher efficiency values compared with the values obtained according to the definition of Hayek et al. [14]. These authors define efficiency in terms of the available irradiance. The manufacturer's efficiency of 80–85% is estimated according to this definition. It is, nonetheless, believed that the acquired results are principally expected.

In decision, the 30° slope is identified as the optimal angle with regard to the various seasons and also fluctuates minimally between the solstices. This angle results in very similar values in March, compared to the 25° angle and yield the highest values in September. It is likely that the 30° slope is also the optimal choice in Pretoria.

8. Conclusions

A numerical model was developed and implemented in Engineering Equation Solver to investigate the performance of a SWH system. The developed model predicted the performance of a practical system within ±3% of the experimental values. This model can, therefore, be used to provide reliable results of a solar water heating system at any given operating conditions. Results from the analysis showed similar trends for the performance at different tilt angles. In summer, the 40° slope pro-

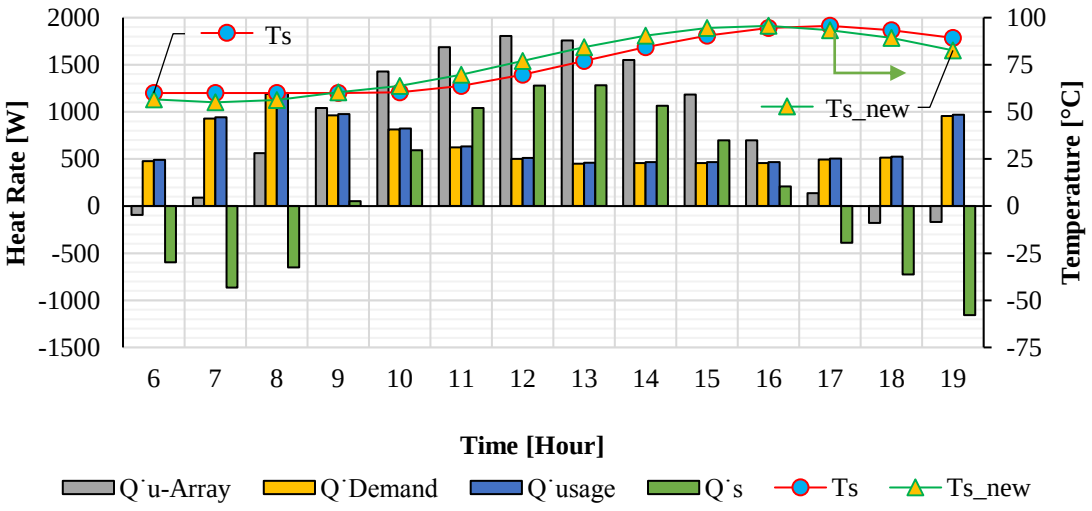

Figure 9: Storage performance trend in solar water-heating application (December).

Table 2: Slope angle maximum performance values.

	March	*June*	*September*	*December*
$\dot{Q}_u$ [W]	1 791.10	1 849.25	1 919.85	1 862.83
T_o [°C]	99.10	90.06	103.98	102.68
Efficiency [%]	92.74	91.43	92.70	92.95
Slope angle (°)	25°	40°	30°	25°

duced the least amount of useful heat and outlet temperature, whereas the 25° slope produced the most. In winter, the opposite was observed, and the 40° slope produced the greater amount. The same inverse seasonal relationships are found for slope angles of 35° and 30°. In autumn and spring, the collector produced similar results during the slope angles with small differences. The optimal seasonal slope angle for a SWH system was identified as 30°. Lastly, a 20-receiver tube collector system operated maximally in September, reaching an outlet temperature of 103.98 °C and yielding a useful heat rate of 1 919.85 W.

Acknowledgements

The support received from the Tshwane University of Technology and the University of the Witwatersrand is acknowledged. The support received from the National Research Foundation is also acknowledged. Special thanks to the South African Weather Service for providing data used in this investigation.

References

1. Eskom. 2015. *COP17 Fact sheet : Solar water heating rebate program* [Online]. Available: http://www.eskom.co.za/AboutElectricity/FactsFigures/Documents/The_Solar_Water_Heating_SWH_Programme.pdf [Accessed 2015/03/09 2015].
2. REN21 2014. Renewable energy 2014 global status report. Paris: REN21 Secretariat.
3. Centre for Renewable and Sustainable Energy Studies and AEE- INTEC. 2014. *The South African solar thermal technology road map* [Online]. Available: www.solarthermalworld.org/sites/gstec/modules/ pubdlcnt/pubdlcnt.php?file=http://www.solarthermalworld.org/sites/gstec/files/story/2014-12-05/solar-thermal-road-map-working-document-3-nov-2014.pdf&nid=63774 [Accessed 2015/03/09].
4. Allouhi, A., Jamil, A., Kousksou, T., Mourad, Y. and Zeraloui, Y. 2015. Solar domestic water heating system in Morocco: An energy analysis. *Energy Conversion and Management,* 92**,** 105-113.
5. Hazami, M., Kooli, S., Naili, N. and Farhat, A. 2013. Long-term performances prediction of an evacuated tube solar water heating system used for single-family households under typical North-African climate (Tunisia) *Solar Energy*, 94**:** 283–298.
6. Mazarron, F. R., Porras-Prieto, C. J., Garcia, J. L. and Benavente, R. M. 2016. Feasibility of active solar water heating systems with evacuated tube collector at different operational temperatures. *Energy Conversion and Management*, 113**:** 16–26.
7. Jafarkazemi, F. and Abdi, H. 2012. Evacuated tube solar heat pipe collector model and associated tests. *Journal of Renewable and Sustainable Energy*, 4**:** 1–13.
8. International Organization for Standardization 1994. ISO 9806-1:1994 Test methods for solar collectors – Part 1: Thermal performance of glazed liquid heating collectors including pressure drop.
9. Jafarkazemi, F., Ahmadifard, K. and Abdi, H. 2016. Energy and exergy of heat pipe evacuated tube solar collectors *Thermal Science*, 20**:** 327–335.
10. Hlaing, S. and Soe, M. M. 2012. Design calculation and heat transfer analysis of heat pipe evacuated tube solar collector for water heating. *International Journal of Science, Engineering and Technology Research (IJSETR)*, 1**,** 1–5.
11. Azad, E. 2008. Theoretical and experimental investigation of heat pipe solar collector. *Experimental Thermal and Fluid Science*, 32**:** 1666–1672.
12. Briel, A. Z. A. and Bunt, E. A. 1994. Optimization of flat plate solar collector angles at a latitude just outside the tropics. *N&O Joernaal*, 10**:** 58–60.
13. Asowata, O., Swart, J. and Pienaar, C. 2012. Optimum tilt angles for photovoltaic panels during winter months in the Vaal triangle, South Africa. *Smart Grid and Renewable Energy*, 3**,** 119 - 125.
14. Hayek, M., Assaf, J. and Lteif, W. 2011. Experimental investigation of the performance of evacuated tube solar collectors under eastern mediterranean climatic conditions. *Energy Procedia*, 6**:** 618–626.
15. Kalogirou, S. A. 2014. *Solar energy engineering processes and systems* Oxford, United Kingdom, Elsevier.
16. Duffie, J. A. and Beckman, W. A. 2013. *Solar engineering of thermal processes,* Canada, John Wiley & Sons.
17. ITS Solar. 2015. *How does an evacuated tube heat pipes collector work?* [Online]. Available: http://www.itssolar.co.za/download.php?file=evac/ITS%20-%20How%20does%20Evacuated%20%20Tubes%20work.pdf [Accessed 2015/08/11].
18. Ng, K. C., Yap, C. and Khor, T. H. 1999. Outdoor testing of evacuated tube heat-pipe solar collectors. *Institution of Mechanical Engineers*, 214 23-30.
19. Cengel, Y. A. and Ghajar, A. J. 2011. *Heat and mass transfer: Fundamentals and applications,* New York, Mc Graw Hill.
20. ITS Solar. 2015. *Evacuated tube specifications* [Online]. ITS Solar. Available: http://www.itssolar.co.za/download.php?file=evac/ITS-10-15-20-Evacuated-Tube-Specifcations.pdf [Accessed 2015/07/21].
21. Solarray. 2015. *High pressure solar water heater catalogue* [Online]. Solarray. Available: http://solarpowergeyser.co.za/high-pressure-solar-water-heater-150-l/ [Accessed 2015/07/22].
22. South African Weather Service 2015. Global, beam and diffuse irradiance of Pretoria, South Africa (January 1957–December 1987)
23. South African Weather Service 2015. Meteorological data of Pretoria UNISA, South Africa (January 2009–December 2014).

24. Meyer, J. P. and Tshimankinda, M. 1996. Domestic hot water consumption in South African townhouses. *Energy Conversion and Management*, 39, 679-684.